International Journal of Advanced Engineering and Management Research

Vol. 6, No. 05; 2021

ISSN: 2456-3676

MODELLING OF THE EFFECTS OF FRICTION ON BULK DEFORMATION BEHAVIOUR DURING DROP-FORGING OF AA7075

W. Tetlow, R.P. Turner
School of Metallurgy & Materials, University of Birmingham, Edgbaston, Birmingham, B15 2TT

Abstract
Aluminium alloy 7075 components are commonplace in the aerospace industry due to their high strength: density ratio. The investigation of the effects of friction during drop forging on the mechanical properties, thermal properties, and grain size of the finished product is carried out and analysed using finite element (FE) modelling. Three different coefficients of friction are simulated, and three different starting soak temperatures simulated in order to predict results across a variety of industrial conditions. The coefficient of friction is predicted to not have a marked effect on grain size and thus mechanical properties of the component - the strengthening is attributed to shear bands and the formation of nanograins. A higher coefficient of friction of 0.7 is predicted to inhibit the material flow of the billet over the die, thus increasing forging time and production cost unnecessarily. Whereas, a low coefficient of friction of 0.12 is predicted to cause high residual stresses as the billet wants to deform around sharper tooling edges during the forging process, with these corners acting as stress raiser locations. This resulted in stress values predicted to approach the tensile strength of AA7075.

Keywords: Aluminium; Finite element; grain; nanograin; shear; recrystallization;

1. Introduction

Drop forged aluminium parts are very commonplace in the aerospace and automotive industries [Zheng, 2018] and are therefore often mass-produced by specialist drop-forging firms. One of the key properties of the aluminium alloys used is their high strength/density ratio [Tajally, 2011], granting them very good mechanical properties whilst remaining lightweight [Deschamps, 1998]. It is therefore of industrial interest to understand any causal relationship between process conditions and emerging component property. Any important or significant trends in the relationships between process parameters and outputted material properties [Rao, 2016] could allow manufacturers to improve understanding of the complex and dynamic thermal and mechanical fields experienced by the deforming workpiece, and so optimise their process to produce higher quality components with improved mechanical properties.

As researched by Weronski., 1999, grain coarsening in aluminium forgings is an important issue as the larger grain size caused by higher strain rates can be categorically linked to the deterioration of mechanical properties [Wang, 2012] throughout the service life of a component [Jin, 2009]. Weronski employed finite element modelling in order to conclude that the final grain diameter depends mainly on strain. It is generally accepted that a sufficient strain is required in order to inhibit grain growth and maintain a fine-grained microstructure. Lim, 1990, reported that the minimum strain required to effectively inhibit grain growth is 15%, and in order to

Vol. 6, No. 05; 2021

ISSN: 2456-3676

consistently reach the acceptable limit of ASTM No. 5 grain size a minimum strain of 30% is needed. Lim also described the effects of too little strain, resulting in the majority of grains recovering 'significantly' during a slow heating.

Lim, 1990, commented that not only is a significant strain needed to achieve the ideal microstructure, but a relatively high temperature is also needed for an Al-Cu alloy. This is corroborated by Zhao, 2019, who reported that the main mechanism of achieving smaller grains is through continuous dynamic recrystallisation (CDRX) [Li, 2008; Zhao, 2019]. In the experiments conducted by Zhao, heating to 400°C was sufficient for a partial recrystallisation, however with a strain rate of $0.005s^{-1}$ a temperature of 450 °C is needed for a full dynamic recrystallization of an Al-Cu alloy. Thus a temperature of 400-450 °C is recommended for this alloy in order to promote smaller grain boundaries and dynamic recrystallisation. The literature in unanimous that small grain size is consistent with enhanced mechanical properties, and that fine grains are achieved with combination of high strain, high temperature and low strain rate [Weronski, 1999; Lim, 1990; Li, 2008].

The coefficient of friction during a forging operation plays an important role in the plastic deformation behaviour of metals as they deform during large-deformation manufacturing processes. This in turn plays an important role in the metallurgical properties such as the eventual grain size, and thus the emerging mechanical properties of the component. It is a material dependence not often considered in literature. Coefficient of friction is a system property rather than a material property, as it depends upon the workpiece material, the tool material, and a lubricating agent, and so the specific combinations desired used are often not used within other research. It is therefore proposed that an optimised coefficient of friction for a drop-forging could be computed using the finite element (FE) method, in order to maximise strain and thus minimise grain size, and so improving the predicted mechanical properties of the component at targeted locations. This is the focus of the work, using commercial finite element software.

2. Modelling Methods

A 2D axi-symmetric workpiece and tooling geometry was created to allow for FE simulation of a hypothetical drop-forging of a compressor disc component. This disc can be seen in Fig. 1. A disc component was desirable for modelling due to its axi-symmetric nature, meaning the FE model could be used in the 2D axi-symmetric mode with 2D elements. The coupled thermo-mechanical finite element program Deform (Version 12.0; 2019) was used for the process modelling activity.

The FE software utilises a Newton-Raphson iterative method in order to solve the associated system of non-linear equations. A purely plastic mode was used, as the elastic deformation is far smaller than plastic deformation in a large deformation process such as this. A representative thermo-physical and flow stress dataset for AA7075 (20-500 °C) was selected from the literature [Prasad, 2015] and from materials properties database [Sente Software, 2021], with data ranges sufficient to cover all experienced temperatures, see Fig. 2. The dies are defined as rigid objects,

Vol. 6, No. 05; 2021

ISSN: 2456-3676

thus prohibiting deformation. This is an acceptable assumption as the tool wear is marginal compared to the deformation of the billet.

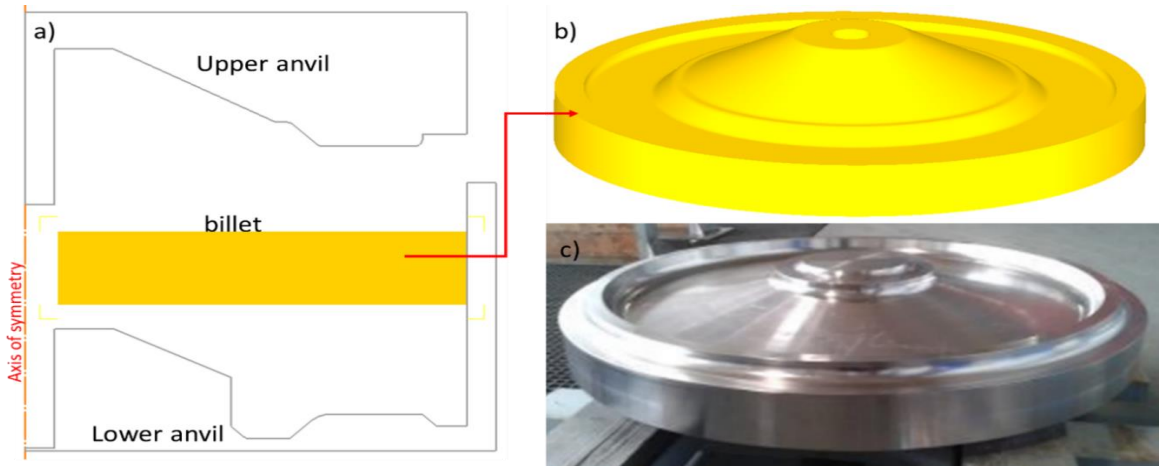

Fig. 1. (a) FE modelling geometry in 2D axi-symmetric, before forging, (b) rendered as a 3D object after drop-forging, and (c) the real compressor disc.

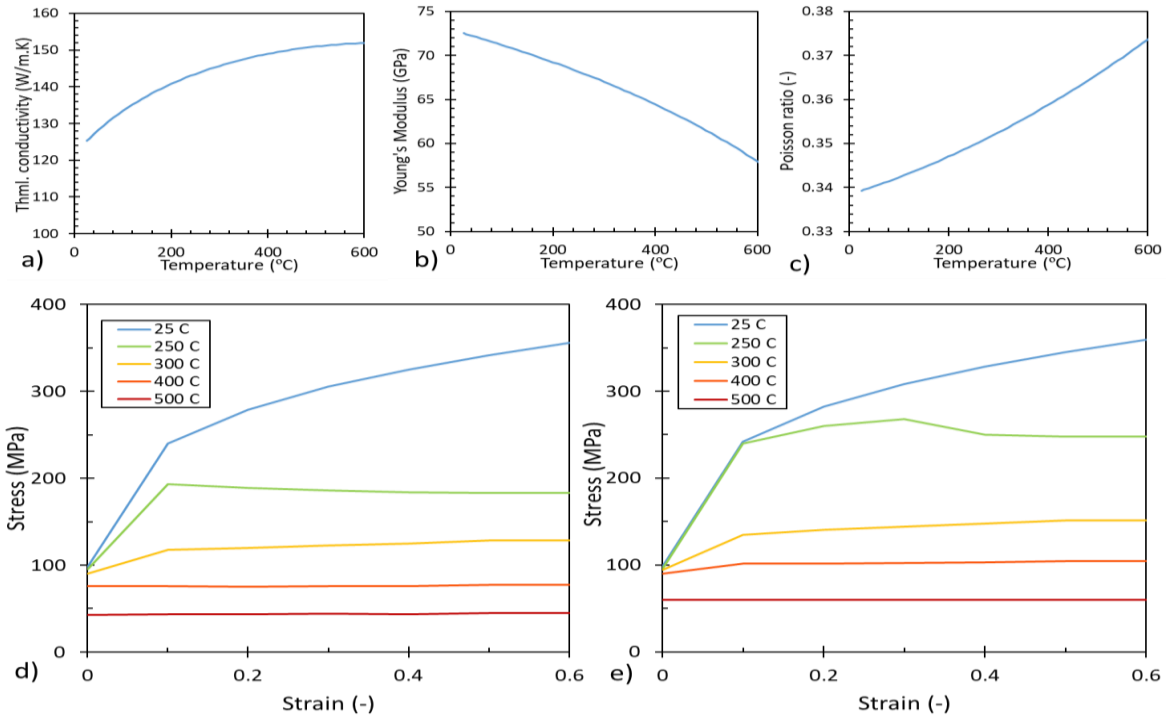

Fig. 2. Temperature-dependent functions for; (a) Thermal conductivity, (b) Young's modulus, (c) Poisson ratio, (d) stress-strain at 0.1/s rate, (e) stress-strain at 1/s rate, for AA7075 [Prasad. 2015, Sente software 2021].

Vol. 6, No. 05; 2021

ISSN: 2456-3676

Thermal boundary conditions are added to the billet in order to simulate accurately the heat loss to the environment and to simulate contact with the dies. The environment temperature is set to 25°C, room temperature, and the convection coefficient is kept at the deform default value of 20W/m^{2}K. The volume of the billet is calculated and maintained constant throughout in order to preserve the mass and reduce any numerical errors during computation. The top die movement type is set to 'hammer' in the software, the hammer energy is inputted as 10800 N.m, and the hammer mass as 630kg [Massey Forging Ltd, 2021]. The blow efficiency is set to 0.75 and kept constant throughout the simulation. Once a hammer blow exhausts all of its energy, the hammer is raised and strikes the billet again, over and over until the forging completely fills the die cavity, as would be the case in reality. The coefficient of friction between the billet and the dies it is set to a differing value of 0.12, 0.3 or 0.7 to represent different lubricated forging conditions [Hill, 2021].

Each time-step is set to 0.001 s; enough time to capture the full deformation of each hammer strike in a few steps. A short mesh sensitivity study was carried out to achieve accurate results in as short a run-time as possible, with an optimised mesh, which yielded results insensitive to the mesh size used. The finalised mesh across the 2D axi-symmetric representation of the 3D object consisted of 4200 elements, and is shown in Fig. 3.

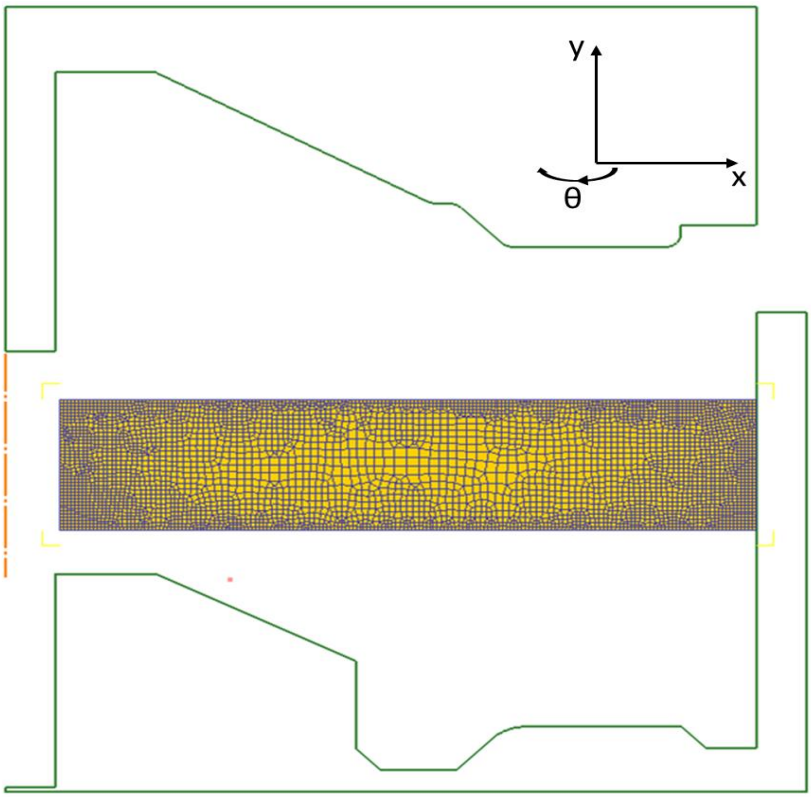

Fig. 3: 2D Mesh used in the 2D axi-symmetric drop - forging modelling

Vol. 6, No. 05; 2021

ISSN: 2456-3676

Associated modelling errors for this hypothetical drop-forging, in the absence of experimental data to validate the predictions, were taken as the small sensitivity to the selected mesh. The resulting associated thermal error of the FE model was 0.5%, whilst the mechanical error was slightly larger, at 6.5%. Once the optimised mesh was known, a series of models was computed according to Table 1. A full-factorial 3x3 matrix of trials, considering two 3-level input parameters; namely the coefficient of friction and the billet start temperature, was simulated. Data could then be gathered about the predicted stress, strain, damage, and temperature of the material before, during and after the drop-forging process.

Table 1. Process parameter variations across the nine Finite Element models

Group	Model No.	Coefficient of friction	Start temperature (^{0}C)
Unlubricated	1	0.7	380
	2	0.7	400
	3	0.7	420
Standard lubrication (eg: Graphite + Water)	4	0.3	380
	5	0.3	400
	6	0.3	420
Excellent lubrication (eg: Carbide insert)	7	0.12	380
	8	0.12	400
	9	0.12	420

3. Results

3.1 Material Flow

Analysis of the predicted thermal and mechanical fields produced from the FE modelling activity, gives rise to a lot of data that can be cross-compared for end-state variations caused by the process parameters. The material flow nets predicted by FE seem almost identical with only some very slight differences between them, see Fig. 4. However, the flow-nets only capture the end-state material flow. Importantly, the simulations of unlubricated forging took more hammer strikes to completely fill the die recess than either of the simulations with a lower coefficient of friction, taking 47 blows to fully deform compared to 43 blows for the other groups at 380°C. As more blows to the billet leads to a greater cooling, so the production takes longer for components with a higher friction value, and this increase could become significant if cooling were such that a secondary heating operation was needed to make the workpiece malleable again.

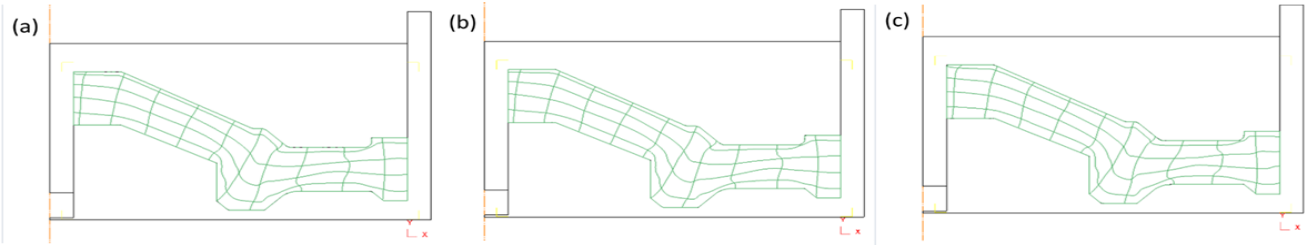

Fig. 4. Material flow-nets for; (a) standard lubrication, (b) carbide insert, (c) unlubricated simulations at 380^{0}C

Vol. 6, No. 05; 2021

ISSN: 2456-3676

3.2 Temperature

To allow for direct comparison for a significant location in the billet, representing both bulk material and interface regions, a series of data points were taken from the cross section to give a representation of areas yielding both high and low deformation, see Fig. 5. This was selected as it covers the two extremes of the forging process, with the interface acting as a 'worst-case scenario'.

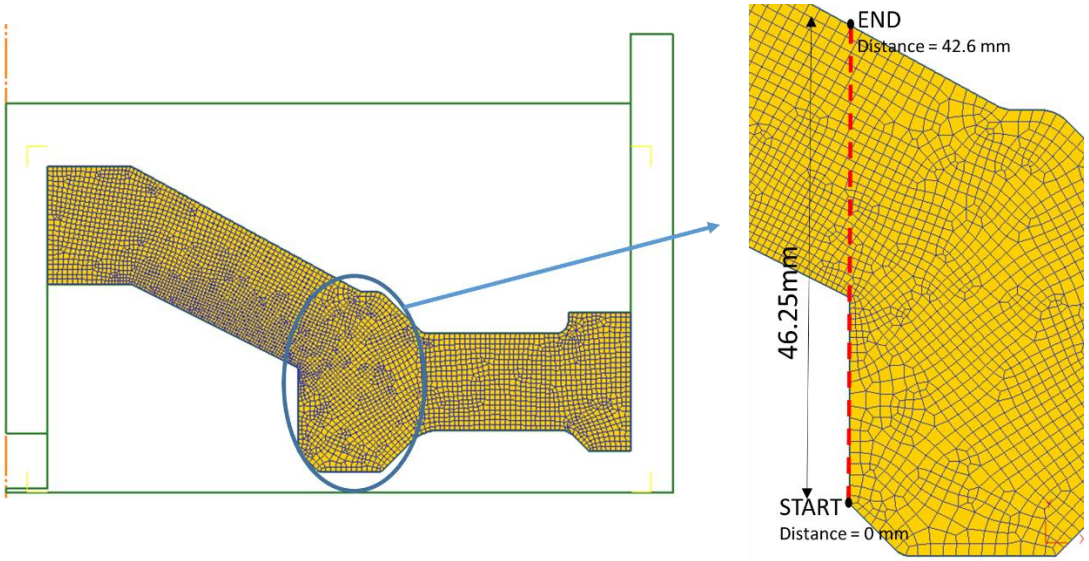

Fig. 5. Location of the nodes analysed for thermal and mechanical fields

The solidus and liquidus temperatures for AA7075 are 480 ^{0}C and 635^{0}C respectively. Thus, one can observe from Fig. 6 that the vast majority of the forged billet is around the temperature range of 410- 460°C, and so will forge successfully. Notably, the peaks of temperature for the unlubricated state are significantly higher, by 100 ^{0}C in places, than the lubricated, and 150 ^{0}C hotter than the carbide insert interface model. The data points at high temperatures within the melting stage for the alloy, in Fig. 7, denote an interface within the forging, and so this is potentially a source of incipient melting. However, given the difficulty in FE prediction of metal to metal interface conditions, so this may be a modelling uncertainty due to overly high friction coefficient, rather than necessarily a real trend. Furthermore, the diagonal streaks of high temperature (Fig. 6) are hypothesised to be due to the formation of shear bands and the associated temperature increase due to internal shear, a trend that will be investigated in the associated mechanical fields.

Vol. 6, No. 05; 2021

ISSN: 2456-3676

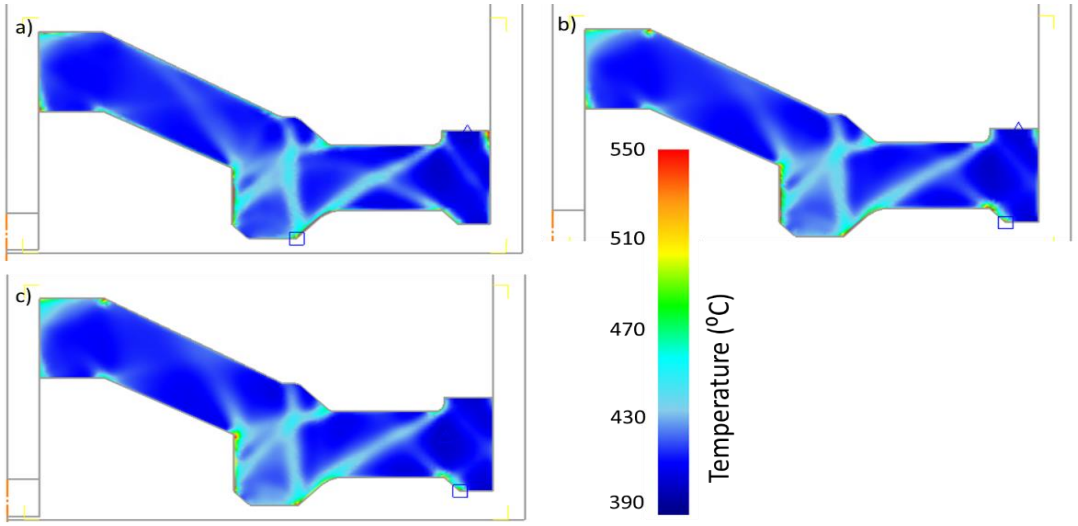

Fig. 6. FE predictions for temperature at end of drop-forging, for models starting at 400 ^{0}C, with (a) unlubricated, (b) lubricated, (c) carbide insert interface conditions.

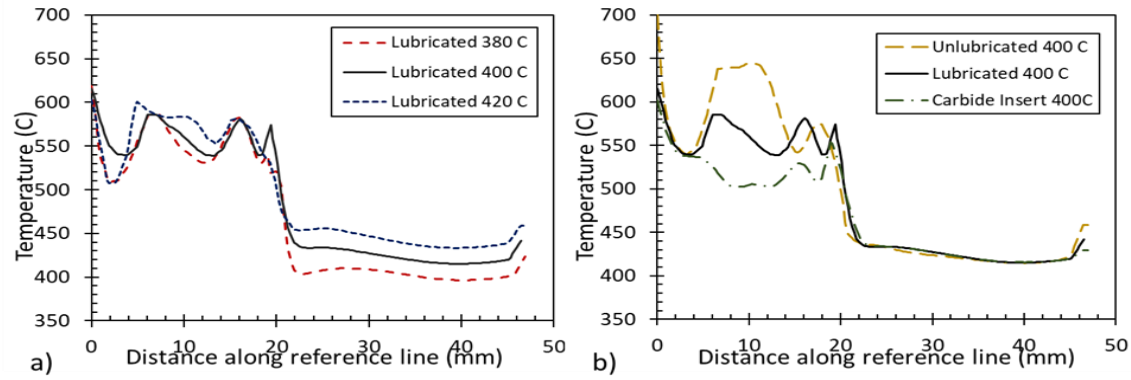

Fig. 7. Impact on predicted finishing billet temperature of; (a) coefficient of friction, (b) start temperature.

3.3 Stress and Strain

The Von Mises stress field was studied, following the Von Mises criterion (Equation 1), where the three stress values given are the stresses in the principal Cartesian directions: x, y and θ.

$$\sigma_{vM} = \sqrt{0.5[(\sigma_1 - \sigma_2)^2 + (\sigma_2 - \sigma_3)^2 + (\sigma_3 - \sigma_1)^2]} \qquad \text{Equation 1}$$

The end-state von Mises stress fields for models varying the coefficient of friction, for the billet starting at 380 ^{0}C, are presented in Fig. 8. It is evident that low friction coefficient simulations (μ = 0.12) are predicted to have the highest average stress of any forging, which is exacerbated at peak stress locations.

Vol. 6, No. 05; 2021

ISSN: 2456-3676

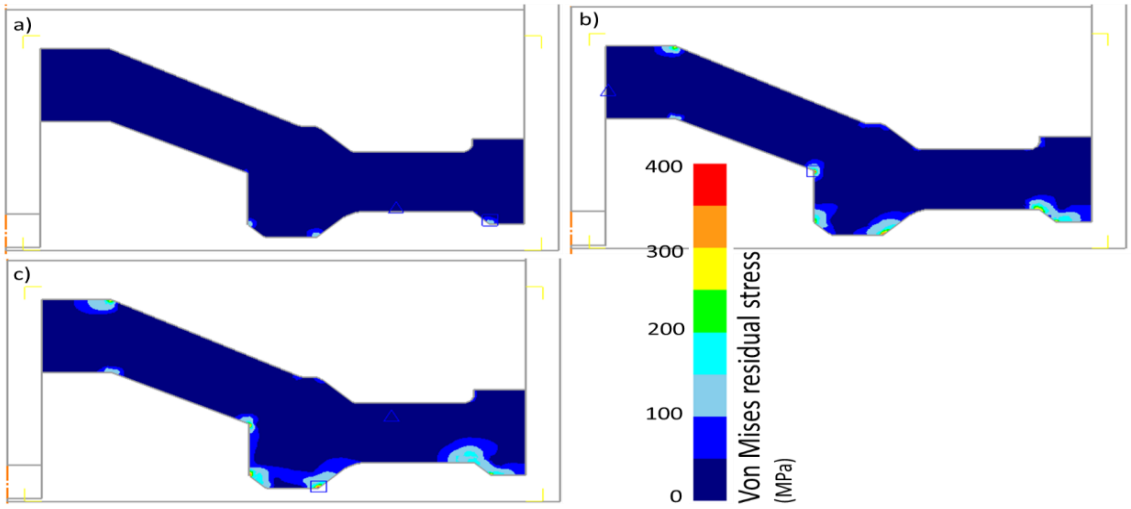

Fig. 8. Von Mises stress fields within the billet for; (a) unlubricated, (b) lubricated, (c) carbide die insert models

It can also be demonstrated by Fig. 9 that high friction unlubricated simulations ($\mu = 0.7$) are predicted to have lower stress values when measured using the same data point line as temperature, especially at peak stress points. The peak stresses in all models is observed at the sharp radii around the edge, highlighting the stress raiser effect of corner regions.

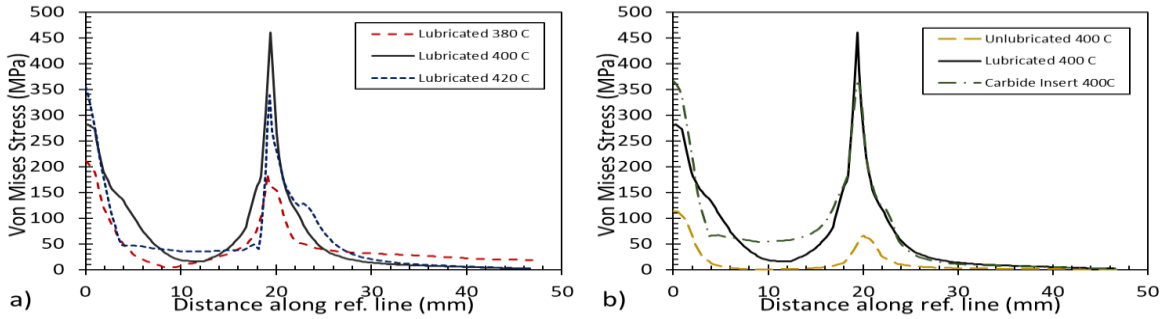

Fig. 9. Effect of (a) initial billet temperature, (b) coefficient of lubrication, on von Mises residual stress

The predicted von Mises strain field had little variation with respect to either input parameter, the initial starting temperature of the forging simulation or the coefficient of friction. Very similar results were obtained at all friction coefficients (for a constant starting temperature) see Fig. 10, and for all temperatures (for fixed friction coefficient), as shown in Fig. 11, with a peak strain of around 1.8, observed at interface regions, and a minimum strain of around 0.4 for all simulations. However, the classical pattern indicative of shear bands, the oblique angle streaks of higher strain, commonly emanating from corner features, are clearly present throughout, again for all initial temperatures and all coefficients of friction.

Vol. 6, No. 05; 2021

ISSN: 2456-3676

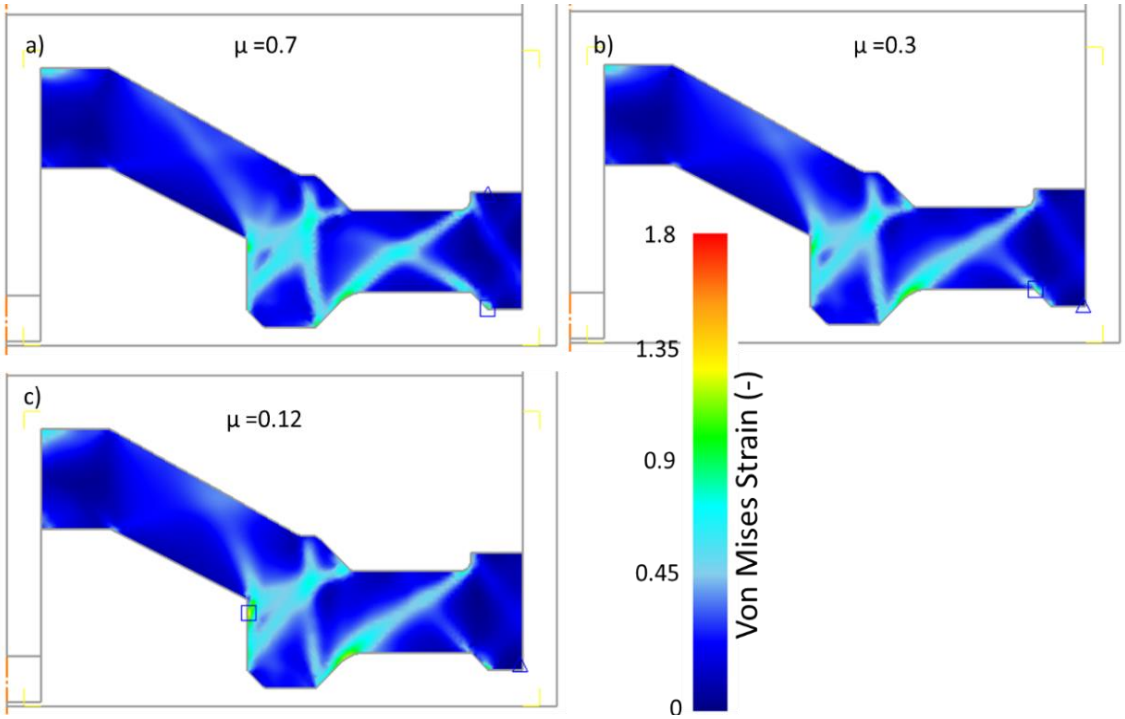

Fig. 10. Von Mises strain fields within the billet for; (a) unlubricated, (b) lubricated, (c) carbide die insert models, starting at 400 ^{0}C.

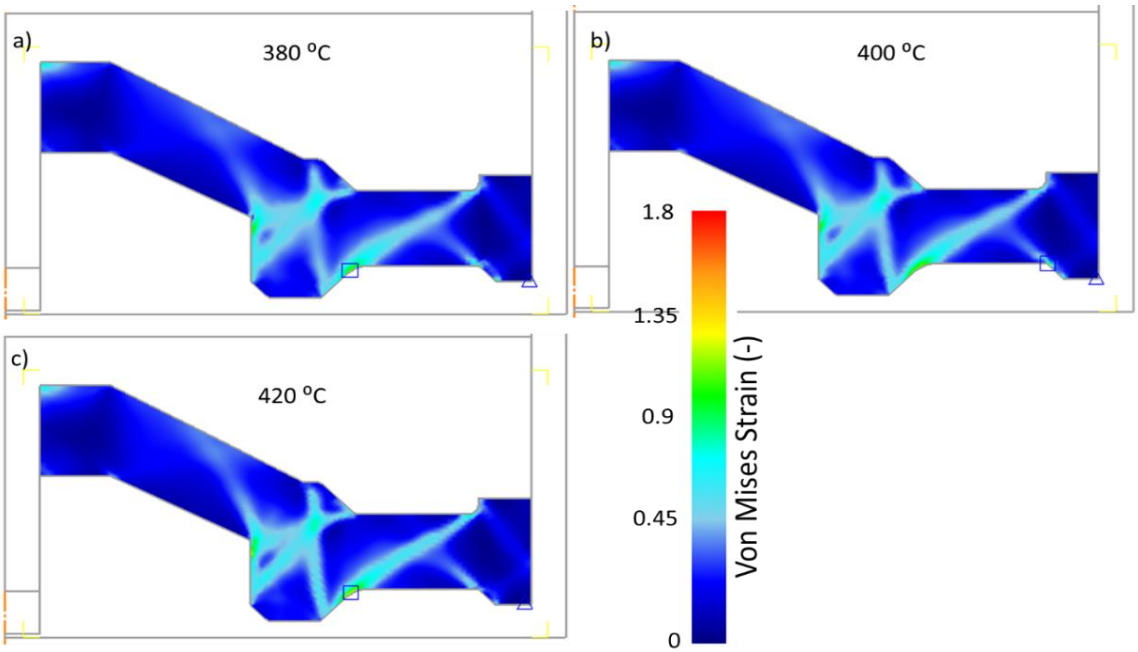

Fig. 11. Von Mises strain fields within the billet starting at; a) 380 ^{0}C, b) 400 ^{0}C, (c) 420 ^{0}C, for models with standard lubrication (μ = 0.3) coefficient of friction

Vol. 6, No. 05; 2021

ISSN: 2456-3676

3.4 Fracture criterion

A normalised Cockroft-Latham fracture criterion, given in Equation 2, was also analysed to understand further mechanical predictions about the billet. The Cockroft - Latham fracture criterion uses the ratio of values for the maximum principal stress and the equivalent strain, to predict the likelihood of any point in the component fracturing at any given time [Stebunov, 2020].

$$C_{norm} = \int^{\varepsilon eff} \frac{\sigma_{max}}{\bar{\sigma}} d\varepsilon_{pl} \qquad \text{Equation 2}$$

Where $\sigma_{max}$is maximum principal stress, $\bar{\sigma}$ is effective stress, ε_{pl} is plastic strain. It gives the modeller an understanding of the likelihood of the billet experiencing fracture at all locations within the billet.

The predicted results follow a similar trend to temperature. As shown in Fig. 12 a very similar finding can be identified for all three initial billet temperatures, whereas there is a more pronounced variation in damage for varying coefficients of friction. However, usually the high friction forgings are still predicted to sustain the most damage, whilst low friction forgings are predicted to have the least. Given that the unlubricated (high coefficient of friction) models marginally had the higher predicted strain, and the dependence of the fracture criterion on strain, it follows that these models will also have the highest damage value (Fig. 12 and Fig. 13). However, given its dependence upon the strain, there is very little variation between fracture damage predicted for the models, despite differences in coefficient of friction or initial temperature. Across all models the damage was at its peak closest to the top die and around the shear bands, which is consistent as these are the areas of high deformation.

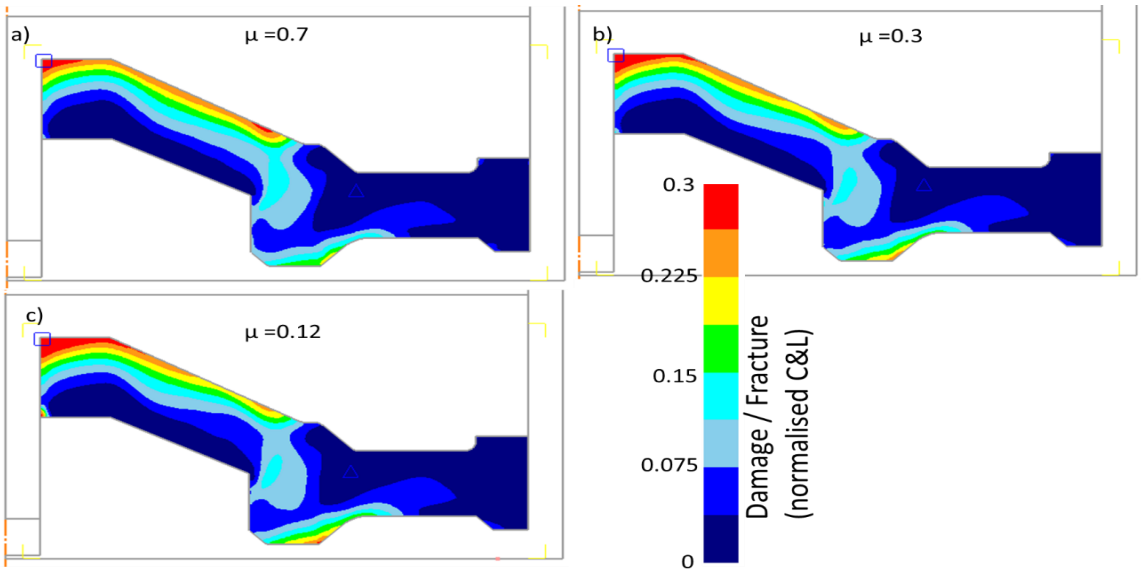

Fig. 12. Normalised Cockroft and Latham fracture criterion parameter within the billet (a) unlubricated, (b) lubricated, (c) carbide die insert models, starting at 400 ^{0}C.

Vol. 6, No. 05; 2021

ISSN: 2456-3676

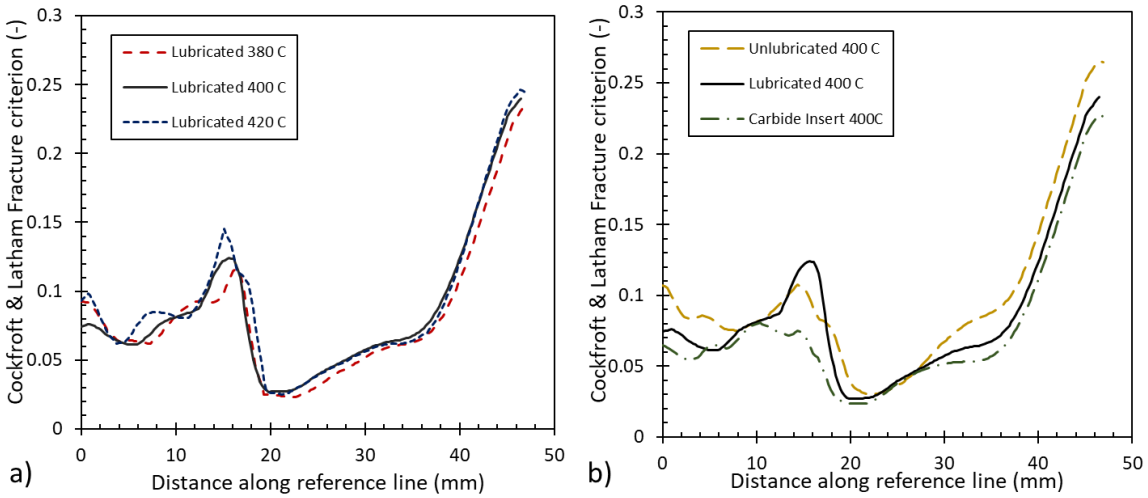

Fig. 13. Effect of (a) initial billet temperature, (b) coefficient of lubrication, on normalised Cockroft and Latham fracture criterion, across the line indicated in Figure 5.

4. Discussion

One of the more interesting features observed within the temperature field and the effective strain field is the diagonal streaks of increased temperature and strain, hypothesised to be indicative of shear band formation, seen in Figures 10-11. A shear band is a strain localisation forming a band-like inhomogeneity, which exclusively forms at oblique angles to the axis of deformation [Yadav, 2020], much like those predicted in this hypothetical forging. Shear bands arise due to rapid deformation generating a lot of heat, which is unable to dissipate into the surrounding material causing a localised softening of material [Pelleg, 2020]. The literature [Li, 2008] describes a number of nanograins observed to form in pure copper during severe plastic deformation. One method of nucleation of nanograins occurred in shear bands and gave the nanograins an average size of 75nm. The average grain size of copper is around 50µm [Wu, 2019] and it is a face-centre cubic material. Similarly, AA7075 is an FCC material, with an average grain size of the same order of magnitude [Dong, 2020] and thus is likely to follow this trend, forming nanograins amidst the shear banding. Having very fine grains aligned with the shear bands could drastically improve the material strength, and having multiple shear bands will eliminate any anisotropy that may arise from having oriented grains.

Figure 8 shows that when predicting Von Mises stress the models using the lowest coefficient of friction are the ones that end up with the highest values of residual stress post-forging, and the models with the highest friction have the lowest residual stresses. It is also evident from Figure 8 that the areas of peak stress are centred around sharp edges in the die that the billet must conform around. Other work in the literature [Ebara, 2008], found during a study of hot forging failures, that corners not having sufficiently large radii was a common cause of failure. The low coefficient of friction allows the billet to flow over the dies more easily during forging, however when flowing over sharp edges the fast deformation appears to cause high residual stress. According to the ASM materials specification [ASM Matweb Inc, 2018] AA7075 has a tensile

Vol. 6, No. 05; 2021

ISSN: 2456-3676

strength of 570MPa, meaning the low friction simulation is at a serious risk of fracturing during forging due to a build-up of stress concentrations.

All of the theoretical forgings simulated in this work predicted the nucleation of adiabatic shear bands throughout the component, which was also demonstrated by the regions of high strain in Figures 10 - 11. It was also demonstrated that the variation in strain is minimal between models of different frictional coefficients and initial billet temperatures, with each group of simulations showing the same trend. This small variation could indicate that the strain during forging was influenced much more by the component geometry than by any other processing parameter, including lubrication of the dies.

5. Conclusion

A finite element simulation of a hypothetical AA7075 forging for aerospace applications was constructed, exploring the impact of the starting temperature and friction coefficient. The following conclusions are drawn.

- Variations in temperature are mainly arising due to the mechanical interface between the billet and the die. Otherwise, the temperature fields are reasonably consistent between billets with different coefficients of friction. Observing changes in temperature (Fig. 10), however, coupled with the changes in strain (Fig. 12) strongly suggests the formation of shear bands, likely containing ‘nanograins’.
- These nanograins increase the strength within the shear band itself, but the grain size mismatch is also theorised to improve mechanical properties with dislocation movement being impeded at the grain/nanograin interface.
- A high coefficient of friction is predicted to take more hammer blows to complete the forging of a component than a lower friction value. This would lead to a higher rate of cooling and potentially a significantly longer production time and thus cost than is necessary were a lower coefficient of friction present.
- Having too low a coefficient of friction could potentially lead to increased risk of fracture during forging, as shown by the predicted tensile stresses reaching values close to the material tensile strength (570MPa) (Fig. 13). Thus a high coefficient of friction between the die and the billet will form nanograins with a very high probability, but more importantly may prevent brittle fracture occurring during the forging process.

References

ASM Matweb Inc., 2018: ASM. Matweb Inc., “Aluminium 7075-t6; 7075-t651 data-sheet.” /. Available: Jul 2021, http://asm.matweb.com/search/SpecificMaterial.asp?bassnum=MA7075T6/ 2018.

Deschamps, 1998: Deschamps, A., Brechet, Y., “Influence of quench and heating rates on the ageing response of an Al-Zn-Mg-(Zr) alloy,” *Materials Science and Engineering A*, 251:(1-2), pp. 200–207, 1998.

Dong, 2020: Dong, Y.F., Ren, B.H., Wang, K,, Wang, J.,. Leng, J.F., "Effects of graphene addition on the microstructure of 7075Al," *Materials Research Express*, 7:(2), 2020.

Ebara, 2008: Ebara R., Kubota, K., "Failure analysis of hot forging dies for automotive components," *Engineering Failure Analysis*, 15:(7), pp. 881–893, 2008.

Hill, 2021: Hill, S., Turner, R., Thermo-mechanical forging of 708M40 steel ring samples: experiments and modelling, *Int J Adv Manuf Technol*, 116:(7); pp. 2577-2590, 2021. https://doi.org/10.1007/s00170-021-07546-w

Jin, 2009: Jin, N., Zhang, H., Han, Y., Wu, W., Chen, J., "Hot deformation behavior of 7150 aluminum alloy during compression at elevated temperature," *Materials Characterization*, 60:(6), pp. 530–536, 2009.

Li, 2008: Li, Y.S., Tao, N., Lu, K., "Microstructural evolution and nanostructure formation in copper during dynamic plastic deformation at cryogenic temperatures," *Acta Materialia*,. 56:(2), pp. 230–241, 2008.

Lim, 1990: Lim, L.C., Fong, H.S., "Excessive grain growth in forged aluminium-base compressor blades," *Journal of Materials Processing Tech*., 23:(2), pp. 211–222, 1990.

Massey Forging Ltd., 2021: Massey Forging Ltd, Croft Street, Hyde, Cheshire, United Kingdom, SK14 1EE.

Pelleg, 1990: Pelleg, J., Fracture in AM and traditional manufactured components; 1st Edition, Elsevier, Netherlands. 2020.

Prasad, 2015: Prasad, Y., Rao, K.,. Sasidhara, S., Hot working guide: A compendium of processing maps; 2nd Edition; ASM International, 2015, Available: Jul 2021, https://www.asminternational.org/documents/10192/1849770/05445G_fm.pdf/.

Rao, 2016: Rao, A.C., Vasu, V., Govindaraju, M., Srinadh, K.V., "Stress corrosion cracking behaviour of 7xxx Al alloys: A literature review," *Transactions of Nonferrous Metals Society of China (English Edition*), 26:(6), pp. 1447–1471, 2016

Sente software, 2021: Sente Software, Surrey Technology Centre, Guildford, United Kingdom GU2 7YG.

Stebunov, 2018: Stebunov, S., Vlasov, A., Biba, N., "Prediction of fracture in cold forging with modified Cockcroft-Latham criterion," *Procedia Manufacturing*, 15, pp. 519–526, 2018.

Tajally, 2011: Tajally, M, Emadoddin, E., "Mechanical and anisotropic behaviors of 7075 aluminum alloy sheets," *Materials and Design*, 32;(3), pp. 1594–1599, 2011.

Vol. 6, No. 05; 2021

ISSN: 2456-3676

Wang, 2012: Wang, M.. Wang, W., Zhou J., Dong, X., Jia, Y. "Strain effects on microstructure behavior of 7050-H112 aluminum alloy during hot compression," *Journal of Materials Science*, 47:(7), pp. 3131–3139, 2012.

Weronski, 1999: Weronski, W., Gontarz A., Pater, Z., "The reasons for structural defects arising in forgings of aluminium alloys analysed using the finite element method," *Journal of Materials Processing Technology*, 93, pp. 90–93, 1999.

Wu, 2019: Wu, Y., Huang, S., Chen, Q., Feng, B., Shu, D., Huang, Z., "Microstructure and Mechanical Properties of Copper Billets Fabricated by the Repetitive Extrusion and Free Forging Process," *Journal of Materials Engineering and Performance*, 28:(4), pp. 2063–2070, 2019.

Yadav, 2019: Yadav, S., Sagapuram, D., "In situ analysis of shear bands and boundary layer formation in metals," *Proceedings of the Royal Society A: Mathematical, Physical and Engineering Sciences*, 476; 2234, 2020.

Zhao, 2019: Zhao, J., Deng, Y, Zhang, J., Ma, Z., Zhang, Y., "Effect of temperature and strain rate on the grain structure during the multidirectional forging of the Al-Zn-Mg-Cu alloy," *Materials Science and Engineering A*, 756, pp. 119– 128, 2019.

Zheng, 2018: Zheng, K, Politis, D.J., Wang, L., Lin, J., "A review on forming techniques for manufacturing lightweight complex-shaped aluminium panel components," *International Journal of Lightweight Materials and Manufacture*, 1;(2), pp. 55–80, 2018.